Onset of synchronization in weighted scale-free networks

Wen-Xu Wang,[1] Liang Huang,[1] Ying-Cheng Lai,[1,2] and Guanrong Chen[3]

[1]*Department of Electrical Engineering, Arizona State University, Tempe, Arizona 85287, USA*
[2]*Department of Physics and Astronomy, Arizona State University, Tempe, Arizona 85287, USA*
[3]*Department of Electronic Engineering, City University of Hong Kong, Hong Kong SAR, China*

We investigate Kuramoto dynamics on scale-free networks to include the effect of weights, as weighted networks are conceivably more pertinent to real-world situations than unweighted networks. We consider both symmetric and asymmetric coupling schemes. Our analysis and computations indicate that more links in weighted scale-free networks can either promote or suppress synchronization. In particular, we find that as a parameter characterizing the weighting scheme is varied, there can be two distinct regimes: a normal regime where more links can enhance synchronization and an abnormal regime where the opposite occurs. A striking phenomenon is that for dense networks for which the mean-field approximation is satisfied, the point separating the two regimes does not depend on the details of the network structure such as the average degree and the degree exponent. This implies the existence of a class of weighted scale-free networks for which the synchronization dynamics are invariant with respect to the network properties. We also perform a comparison study with respect to the onset of synchronization in Kuramoto networks and the synchronization stability of networks of identical oscillators. © *2009 American Institute of Physics.*
[DOI: 10.1063/1.3087420]

Understanding synchronization in complex networks of large numbers of interacting oscillators is important for areas ranging from communication to biology. How network properties affect the synchronization dynamics has been an issue of active research in recent years. In real-world networks, the interactions among oscillators are often asymmetric and nonuniform. This has motivated research on synchronization in weighted complex networks. Previous studies on this topic focused on the synchronizabilities of networks of identical oscillators, for which the approach of eigenvalue analysis is applicable. However, in realistic networked systems, node dynamics can be nonidentical. There is thus a need to study synchronization in weighted complex networks with heterogeneous node dynamics. Here, we use the Kuramoto model to address this problem. We consider both symmetric and asymmetric weighting schemes and obtain analytic predictions concerning the synchronization properties of the network. Our analysis and computations indicate that more links in weighted scale-free networks can either promote or, counterintuitively, suppress synchronization. A finding is that, regardless of the coupling scheme, two regimes with the opposite synchronization behaviors are separated by a point, at which the onset of network synchronization does not depend on the link density. This then implies the existence of a class of weighted scale-free networks for which the synchronization dynamics are invariant with respect to network connectivity.

I. INTRODUCTION

Synchronization in large networked systems has been an active area of research in statistical and nonlinear physics[1,2] since the pioneering work of Kuramoto.[3] Given a network of coupled nonlinear oscillators, Kuramoto focused on the phase variables and derived a model of phase-coupled oscillators,

$$\dot{\theta}_i = \omega_i + \varepsilon \sum_{j=1}^{N} C_{ji} \sin(\theta_j - \theta_i), \qquad (1)$$

where θ_i and ω_i are the phase and the natural frequency of oscillator i, respectively, $N \gg 1$ is the total number of oscillators, ε is a global coupling parameter that is identical for all oscillators, and $\{C_{ij}\}$ is the coupling matrix. In the model, each oscillator, when isolated, is characterized by a uniform rotation of a given frequency. The frequencies of all oscillators are drawn from a probability distribution $g(\omega)$ with a single maximum at zero. The interactions among the oscillators are described by nonlinear coupling terms. The model is thus relatively simple but highly nontrivial in the sense that it captures many generic features of the dynamics of realistic oscillator networks. A particularly appealing feature of the model is that it is amenable to analysis partly because of the simple node dynamics. In addition, because of the different intrinsic frequencies associated with the oscillators, the isolated node dynamics are not identical but heterogeneous. The model thus enables the problem of synchronization of large networks of heterogeneous elements to be addressed. Indeed the Kuramoto model has been a paradigm for obtaining analytic insights into a variety of synchronization phenomena in physics and biology, as well as in engineering and technology.[4,5]

The coupling scheme in the original Kuramoto paradigm is all-to-all.[3,4] The network is thus densely connected, so the standard mean-field theory can be used to analyze the tran-

sition to synchronization. More specifically, let ε be a global coupling parameter and $R \geq 0$ be an order parameter, where a nonzero value of R indicates certain degree of coherence among the dynamics of the coupled oscillators. A mean-field treatment usually gives ε_c, the critical coupling value at which R starts to increase from zero, or the transition to *partial* synchronization. Recently, the Kuramoto model has been adopted to networks of complex topologies.[6,7] For example, transition to synchronization in scale-free networks[8] has been investigated with predictions for ε_c under both mutual and directed coupling schemes.[6] At the onset, partial synchronization emerges in the form of small synchronous clusters. Mean-field theory predicts that ε_c is determined by the frequency distribution of the phase oscillators and the first two moments of the node-degree distribution. The onset of global synchronization where all oscillators begin to synchronize in complex clustered networks has also been considered.[7]

In this paper, we investigate the transition to synchronization in *weighted* scale-free networks under the Kuramoto paradigm. Our goal is to understand, *quantitatively*, the influence of weighting on the onset of synchronization. Such a network model takes into account the nonuniform interactions among nodes in the network and is therefore believed to better describe large networked systems in reality. Usually, there is a correlation between the weight distribution and the network topology.[9] For scale-free networks, due to the algebraic degree distribution, the weights can be highly heterogeneous, far beyond those in the Boolean representation.[9] Synchronization in weighted scale-free networks has been investigated recently where all existing works assume identical node dynamics and are mostly based on the eigenvalue analysis.[2] Our approach is to use the formula for transition to synchronization in Ref. 6 as a theoretical tool to derive explicit expressions for ε_c for different weighting schemes. To be as general as possible, we shall consider both symmetric and asymmetric couplings.

The main results of this paper can be stated in terms of the dependence of ε_c on some parameter α that characterizes the weighted coupling scheme and controls the degree of homogeneity in link weights. We find that for both symmetric and asymmetric weighted networks, the dependence of ε_c on α is approximately exponential but with different rates for different densities of links even when the network size and the topological parameter are the same. As a result, there exists a critical point α_c such that for $\alpha < \alpha_c$, networks of sparser linkage are more synchronizable than networks of denser linkage in the sense that the critical values ε_c required for partial synchronization in the former case are less than those in the latter case, whereas the opposite holds for $\alpha > \alpha_c$ [Figs. 3 and 4]. The striking phenomenon is that the synchronization dynamics of networks with values of α in the vicinity of α_c are *invariant* with respect to changes in the network link density, and the value of ε_c at α_c is independent of the network structural details. In both the $\alpha < \alpha_c$ and the $\alpha > \alpha_c$ regimes, the network connectivity changes little in the sense that links associated with larger-degree nodes are assigned with smaller weights, but the synchronization dynamics are qualitatively different in the two regimes. In general,

this phenomenon can be attributed to the complex interplay between network structure and dynamics. The phenomenon is predicted analytically with solid numerical support.

A result in Ref. 6 is that for random networks with some prescribed degree distribution, the critical coupling strength ε_c for transition to synchronization is determined by the largest eigenvalue of the adjacency matrix. We will also use this eigenvalue approach to investigate the onset of synchronization in weighted networks to provide additional support for our results. In addition, we will compare results for the onset of synchronization in the Kuramoto network with those from the analysis of synchronization stability in networks of identical oscillators with the same topology.

In Sec. II, we describe our network model with both symmetric and asymmetric weighted coupling schemes. In Sec. III, we provide theoretical and numerical results with respect to the order parameter near the onset of synchronization and ε_c. An eigenvalue analysis for the critical coupling strength is presented in Sec. IV, providing additional support for the generality of our findings. In Sec. V, the dynamics of weighted Kuramoto networks are compared with the dynamics of networks of identical oscillators with the same coupling scheme. Conclusions and discussions are offered in Sec. VI.

II. MODEL DESCRIPTION

We construct scale-free networks by using the standard preferential-attachment model.[8] At each time step, a new node with m links is added and preferentially attached to m existing nodes with probability proportional to the degrees of the existing nodes. Degree distributions of the networks are given by $P(k) \sim k^{-3}$, the minimum node degree of the networks is m, and the average degree is $2m$. We then assign weights to links in terms of the node degrees. Two types of schemes are considered.

(1) Symmetric coupling. We assume the weight associated with the link between nodes i and j to be $w_{ij} = (k_i k_j)^\alpha$, where k_i and k_j are the degrees of i and j, respectively, and α is a control parameter. The coupling strength C_{ij} between nodes i and j becomes $C_{ij} = A_{ij} w_{ij}$, where $\{A_{ij}\}$ is the adjacency matrix of the network. As a result, the coupling strength is symmetric: $C_{ij} = C_{ji}$. This weighted scheme is supported by empirical data of some real-world weighted networks.[9]

(2) Asymmetric coupling. If the directional couplings between two connected nodes are asymmetric, the network will typically be weighted and directed. The weight from node i to node j is $w_{ij} = k_i^\alpha$, but $w_{ij} \neq w_{ji} = k_j^\alpha$ for $k_i \neq k_j$. The coupling matrix element from node i to node j is $C_{ij} = A_{ij} w_{ij}$. This choice of the weighting scheme is motivated by the fact that in certain real-world networks, the weight of a node has a nonlinear correlation with its degree in the form $s_i \sim k_i^\alpha$, where s is the node weight.[9] The asymmetric coupling scheme takes into account both the nonlinear correlation and the fact that the influences from a node to its neighbors are the same.

A global order parameter can be defined to quantify the degree of coherence in the network,[6]

$$r = \frac{\sum_{n=1}^{N} r_n}{\sum_{n=1}^{N} d_n}, \tag{2}$$

where the local order parameter r_n is defined as

$$r_n e^{i\psi_n} = \sum_{m=1}^{N} C_{mn} \langle e^{i\theta_m} \rangle_t. \tag{3}$$

In Eq. (3), ψ_n is the phase associated with the order parameter and $\langle \cdot \rangle_t$ denotes the average over time t. The local total coupling strength of node n is given by

$$d_n = \sum_{m=1}^{N} C_{mn}, \tag{4}$$

where, for a directed network, the subscript mn indicates that the coupling is from node m to node n. When the phase oscillators are not synchronized, the order parameter r has near-zero values; whereas if the oscillators are fully synchronized, r becomes unity. In between the two extreme states, oscillators are partially synchronized. The onset of partial synchronization can be identified by a sudden and rapid increase in the value of r from zero. The order parameter r thus quantifies the degree of phase coherence among the oscillators in the network.

III. EFFECT OF WEIGHTS ON SYNCHRONIZATION

For the Kuramoto model, a general formula for ε_c, the critical coupling parameter for the onset of synchronization, has been obtained previously,[6,10] as follows:

$$\varepsilon_c = \beta_1 \eta_1 = \begin{cases} \beta_1 \langle d \rangle / \langle d^2 \rangle, & \text{symmetric coupling} \\ \beta_1 \langle d^{\text{in}} \rangle / \langle d^{\text{in}} d^{\text{out}} \rangle, & \text{asymmetric coupling,} \end{cases} \tag{5}$$

where $\beta_1 = 2/[\pi g(0)]$, $\langle \cdot \rangle$ stands for the average over nodes in the network, d is the total local coupling strength, and d_n^{in} and d_n^{out} are total local incoming and outgoing coupling strengths, respectively. The value of the order parameter r is given by

$$r^2 = \frac{\eta_2}{\beta_1^2 \beta_2} \left(\frac{\varepsilon}{\varepsilon_c} - 1 \right) \left(\frac{\varepsilon}{\varepsilon_c} \right)^{-3}, \tag{6}$$

where for $\varepsilon \geq \varepsilon_c$, $\beta_2 = -\pi g''(0)\beta_1/16$. For symmetric coupling, η_2 is given by

$$\eta_2 = \frac{\langle d^2 \rangle^3}{\langle d^4 \rangle \langle d \rangle^2}. \tag{7}$$

For asymmetric coupling, we have

$$\eta_2 = \frac{\langle d^{\text{in}} d^{\text{out}} \rangle^3}{\langle (d^{\text{in}})^3 d^{\text{out}} \rangle \langle d^{\text{in}} \rangle^2}. \tag{8}$$

For heterogeneous coupling, ε can be regarded as a nominal coupling parameter. In this case, formulas (5)–(8) are still applicable. To analyze the effect of weighted coupling on the onset of synchronization, we set out to calculate the various averaged quantities in Eqs. (5)–(8).

A. Symmetric coupling scheme

To obtain the critical coupling strength from Eq. (5) requires that the total local coupling strength be calculated, which then yields η_1. We start by rewriting d_i as

$$d_i = \sum_{j=1}^{N} C_{ij} = \sum_{j=1}^{N} A_{ij}(k_i k_j)^\alpha$$

$$= k_i^\alpha \sum_{j=1}^{N} A_{ij} k_j^\alpha = k_i^{\alpha+1} \sum_{k'=k_{\min}}^{k_{\max}} P(k'|k_i) k'^\alpha,$$

where $P(k'|k_i)$ is the conditional probability that a node of degree k_i has a neighbor of degree k'. For a network without degree-degree correlation, we have $P(k'|k_i) = k'P(k')/\langle k \rangle$, where $P(k')$ is the degree distribution of the network. This can be understood by noting that a node of degree k' will be counted k' times as a neighbor of some other nodes in the network. We thus have

$$d_i = k_i^{\alpha+1} \sum_{k'=k_{\min}}^{k_{\max}} P(k'|k_i) k'^\alpha$$

$$= k_i^{\alpha+1} \sum_{k'=k_{\min}}^{k_{\max}} \frac{k'^{\alpha+1} P(k')}{\langle k \rangle} = \frac{k_i^{\alpha+1} \langle k^{\alpha+1} \rangle}{\langle k \rangle}, \tag{9}$$

where the identity

$$\sum_{k'=k_{\min}}^{k_{\max}} k'^{\alpha+1} P(k') = \langle k^{\alpha+1} \rangle$$

has been used. Taking the ensemble average of d_i, we obtain

$$\langle d \rangle = \frac{1}{N} \sum_{i=1}^{N} \frac{k_i^{\alpha+1} \langle k^{\alpha+1} \rangle}{\langle k \rangle} = \frac{\langle k^{\alpha+1} \rangle^2}{\langle k \rangle}. \tag{10}$$

Similarly, the ensemble average of d_i^2 is

$$\langle d^2 \rangle = \left\langle \left(\sum_{j=1}^{N} A_{ij} k_i^\alpha k_j^\alpha \right)^2 \right\rangle$$

$$= \left\langle \left(k_i^{\alpha+1} \sum_{k'=k_{\min}}^{k_{\max}} \frac{k'^{\alpha+1} P(k')}{\langle k \rangle} \right)^2 \right\rangle$$

$$= \left\langle \frac{k_i^{2\alpha+2} \langle k^{\alpha+1} \rangle^2}{\langle k \rangle^2} \right\rangle = \frac{\langle k^{2\alpha+2} \rangle \langle k^{\alpha+1} \rangle^2}{\langle k \rangle^2}. \tag{11}$$

The critical coupling parameter can be written as

$$\varepsilon_c = \beta_1 \frac{\langle d \rangle}{\langle d^2 \rangle} = \beta_1 \frac{\langle k \rangle}{\langle k^{2\alpha+2} \rangle}, \tag{12}$$

where for any given value of μ, $\langle k^\mu \rangle$ can be approximated by $\int_{k_{\min}}^{k_{\max}} k^\mu P(k) dk$. For a scale-free network, the degree distribution can be written as $P(k) = ck^{-\gamma}$, where c is given by
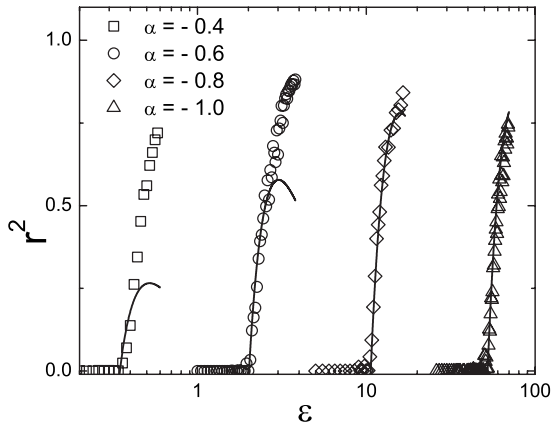
FIG. 1. For an ensemble of standard scale-free networks of $N=2000$ nodes and average degree $\langle k \rangle = 60$, squared order parameter r^2 as a function of global coupling strength ε for different values of the weighting parameter α. The coupling scheme is symmetric. Each data point is obtained by averaging over 20 network realizations. Curves are theoretical predictions given by Eq. (17). Due to the finite-size effect, the algebraic exponent γ in the degree distribution is slightly lower than 3. Here, we use $\gamma \approx 2.9$ in Eq. (17) to draw the theoretical curves.
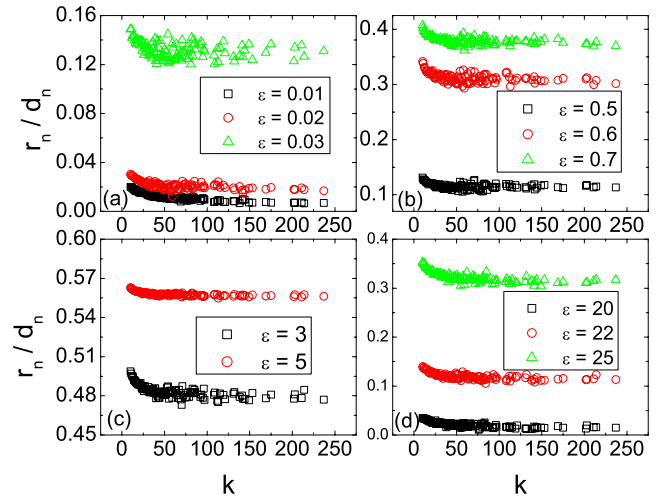

FIG. 2. (Color online) Nodal order parameter r_n/d_n as a function of node degree k for (a) $\alpha = 0$, (b) $\alpha = -0.4$, (c) $\alpha = -0.6$, and (d) $\alpha = -1.0$ for different values of ε close to the onset of partial synchronization. The network size is 2000 and the average degree is $\langle k \rangle = 20$.

$$c = (\gamma - 1)k_{\min}^{\gamma-1},$$

as a result of the normalization condition $\int_{k_{\min}}^{\infty} P(k)dk = 1$ (assuming $\gamma \neq 1$). The maximum degree of the network is determined by $\int_{k_{\max}}^{\infty} P(k)dk = 1/N$, from which we obtain $k_{\max} = k_{\min} N^{1/(\gamma-1)}$. The ensemble-averaged value of k^{μ} can thus be calculated as

$$\langle k^{\mu} \rangle = \int_{k_{\min}}^{k_{\max}} k^{\mu} P(k)dk = \frac{\gamma-1}{\mu-\gamma+1} k_{\min}^{\mu} (N^{(\mu-\gamma+1)/(\gamma-1)} - 1),$$

(13)

which is valid for $\mu - \gamma \neq -1$. Inserting this result into Eq. (12), we get

$$\epsilon_c = \frac{2}{\pi g(0)} \frac{2\alpha+3-\gamma}{2-\gamma} \frac{1}{k_{\min}^{2\alpha+1}} \frac{N^{(2-\gamma)/(\gamma-1)} - 1}{N^{(2\alpha+3-\gamma)/(\gamma-1)} - 1}.$$

(14)

The order parameter can be calculated in a similar way. In particular, from Eq. (7), we have

$$\eta_2 = \frac{\langle d^2 \rangle^3}{\langle d^4 \rangle \langle d \rangle^2}$$

$$= \left(\frac{\langle k^{2\alpha+2} \rangle \langle k^{\alpha+1} \rangle^2}{\langle k \rangle^2} \right)^3 \Bigg/ \left[\frac{\langle k^{4\alpha+4} \rangle \langle k^{\alpha+1} \rangle^4}{\langle k \rangle^4} \left(\frac{\langle k^{\alpha+1} \rangle^2}{\langle k \rangle} \right)^2 \right]$$

$$= \frac{\langle k^{2\alpha+2} \rangle^3}{\langle k^{4\alpha+4} \rangle \langle k^{\alpha+1} \rangle}.$$

(15)

Using Eq. (13), we can express η_2 as

$$\frac{(4\alpha-\gamma+5)(\alpha-\gamma+2)^2}{(2\alpha-\gamma+3)^3}$$

$$\times \frac{(N^{(2\alpha-\gamma+3)/\gamma-1} - 1)^3}{(N^{(4\alpha-\gamma+5)/\gamma-1} - 1)(N^{(\alpha-\gamma+2)/\gamma-1} - 1)^2}.$$

(16)

Finally, we obtain

$$r^2 = -\eta_2 \frac{g''(0)}{2\pi^2 g^3(0)} \left(\frac{\varepsilon}{\varepsilon_c} - 1 \right) \left(\frac{\varepsilon}{\varepsilon_c} \right)^{-3},$$

(17)

where ε_c is given by Eq. (14).

We now provide numerical support for our theoretical predictions [Eqs. (14) and (17)]. The frequency distribution of the phase oscillators is chosen (somewhat arbitrarily) to be $g(\omega) = 3(1-\omega^2)/4$ for $|\omega| \leq 1$ and $g(\omega) = 0$ otherwise. Thus $\beta_1 = 8/(3\pi)$ and $g''(0) = -3/2$. Four curves of r^2 versus ε, corresponding to four different values of the weighting parameter α, are shown in Fig. 1 for ε in the vicinity of ε_c. For each value of α, the order parameter r is approximately zero for $\varepsilon < \varepsilon_c$. At ε_c, r starts to increase from zero, signifying a transition to partial synchronization. The transition point depends on the weighting parameter α. We see that ε_c increases as α decreases, indicating that partial synchronization is more difficult to achieve as α becomes more negative. A larger negative value of α stipulates that links between larger-degree nodes be less weighted, effectively making the network more homogeneous. The results in Fig. 1 thus suggest that homogeneous weights actually hinder synchronization. Equivalently, a heterogeneous weighting scheme tends to facilitate the transition to synchronization. This is somewhat different from the result of eigenvalue analysis of global synchronization in oscillator networks of identical node dynamics, where heterogeneity has been found to suppress synchronization.[1] This seeming "paradox" can be resolved by noting that our analysis yields information about the transition to partial synchronization only, while the eigenvalue analysis is for the global synchronizability of the underlying network. In all four cases, we observe satisfactory agreement between the numerical and theoretical values of ε_c. For $\varepsilon \gtrsim \varepsilon_c$, the agreement between the numerical and theoretical values of the order parameter is also good. It should be remarked that the empirical results of Ref. 9 suggest a value of $\alpha = 0.5$, which is different from the crossover point $\alpha = -0.5$ for the onset of synchronization on weighted networks.

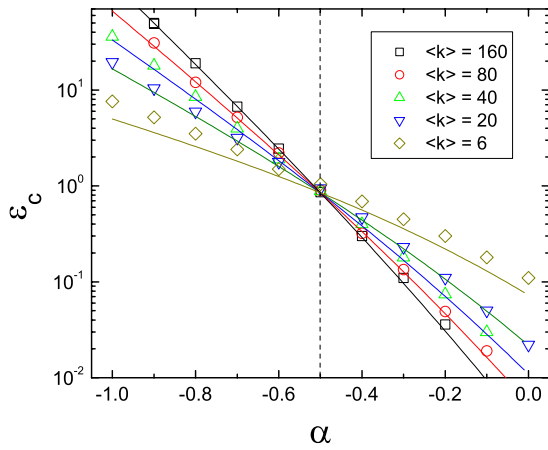The results in Fig. 2 raise the question as to which nodes

FIG. 3. (Color online) For symmetric coupling scheme, critical global coupling strength ε_c as a function of the weighting parameter α for different values of the average degree $\langle k \rangle$. The common intersecting point for different cases occurs at $\alpha = -0.5$ and is marked by the vertical dash line. This point defines two regimes: (i) $\alpha < -0.5$, the abnormal synchronization regime, where networks with more links are less synchronizable, and (ii) $\alpha > -0.5$, the normal regime, where the opposite that more links tend to facilitate synchronization. Data points are from simulations and the curves are analytical results given by Eq. (14). Other parameters are the same as those in Fig. 1.

contribute more significantly to the emergence of partial synchronization. To address this question, we study the dependence of the nodal order parameter r_n/d_n on degree k at the onset of synchronization. As shown in Fig. 2, for different values of α and for ε close to the onset of synchronization, lower-degree nodes tend to be more responsible for the emergence of partial synchronization, regardless of whether node strengths are heterogeneous or homogeneous. This is somewhat counterintuitive for the case of heterogeneous nodal strengths because high-strength nodes and their neighbors are expected to first synchronize. This phenomenon can be explained by noting that the nodal order parameter is normalized by the node strength d_n. Although high-degree nodes can synchronize with some of their neighbors more easily,[11] their contributions to the global order parameter are smaller due to the normalization over their strengths.

Another phenomenon observed from Fig. 1 is that heterogeneous strength distribution (corresponding to higher values of α) tends to facilitate the onset of partial synchronization since lower values of ε_c are required. This can be explained by noting that the total coupling strength among all nodes, $\Sigma_{i=1}^{N} d_i = N \langle k^{\alpha+1} \rangle^2 / \langle k \rangle$, is a decreasing function of α. This means that a larger value of the total coupling strength is associated with more heterogeneous strength distribution, which generally requires smaller values of the global coupling ε_c to achieve partial synchronization. Thus, that heterogeneous strength distribution favors the emergence of partial synchronization can be ascribed to the behavior of the total coupling strength.

The critical coupling strength ε_c as a function of the weighting parameter α for different values of the average degree is shown in Fig. 3 on a semilogarithmic scale. We observe that the dependence of ε_c on α is approximately exponential but the exponential rate is different for different values of $\langle k \rangle$. As a result, two different curves will intersect

at some value of α. A remarkable phenomenon is that *all curves apparently intersect at the same point*! In Fig. 3, the intersecting point is $\alpha_c = -0.5$. There are two consequences. First, for $\alpha = \alpha_c$, networks with different values of $\langle k \rangle$ share the same critical point of transition to synchronization. Second, the dependence of ε_c on $\langle k \rangle$ shows opposite trends for $\alpha < \alpha_c$ and $\alpha > \alpha_c$. In particular, for $\alpha < \alpha_c$, networks with smaller values of $\langle k \rangle$ exhibit smaller values of ε_c and thus are more synchronizable. This is quite counterintuitive, as the results suggest that networks with more links are less synchronizable. We call $\alpha < \alpha_c$ the *abnormal* synchronization regime. For $\alpha > \alpha_c$, the values of ε_c required for synchronization are smaller for larger values of $\langle k \rangle$, indicating that networks with more links are more synchronizable. This is then the *normal* synchronization regime.

The existence of a common intersecting point among the $\varepsilon_c \sim \alpha$ curves for different values of $\langle k \rangle$ can be explained by Eq. (14). For scale-free networks, the minimum degree k_{min} is positively correlated with the average degree $\langle k \rangle$. For example, for the standard scale-free network model we use here, $\langle k \rangle = 2 k_{min}$. In Eq. (14), for $\alpha = -0.5$, $k_{min}^{2\alpha+1} = 1$, indicating that ε_c is independent of both k_{min} and $\langle k \rangle$. Because the intersecting point is common for α_c, the two regimes (i.e., $\alpha < -0.5$ and $\alpha > -0.5$) exhibit a reverse relationship between ε_c and $\langle k \rangle$. The common intersecting point $\varepsilon_c(\alpha = -0.5)$ can actually be calculated by inserting $\alpha = -0.5$ into Eq. (14). We have

$$\varepsilon_c(\alpha = -0.5) = \frac{2}{\pi g(0)}. \tag{18}$$

This value depends only on the frequency distribution of oscillators not on values of quantities such as the weighting parameter α, the exponent of the degree distribution, and the average degree $\langle k \rangle$.

B. Asymmetric coupling scheme

For the asymmetric coupling scheme, the coupling matrix is given by $C_{ij} = A_{ij} k_i^{\alpha}$. The value of ε_c for the onset of synchronization can be derived from Eq. (5). The average incoming coupling value becomes

$$\langle d_{in} \rangle = \left\langle \sum_{j=1}^{N} A_{ji} k_j^{\alpha} \right\rangle = \left\langle k_i \sum_{k'=k_{min}}^{k_{max}} \frac{k' P(k') k'^{\alpha}}{\langle k \rangle} \right\rangle$$

$$= \left\langle \frac{k_i \langle k^{\alpha+1} \rangle}{\langle k \rangle} \right\rangle = \langle k^{\alpha+1} \rangle. \tag{19}$$

The average outgoing coupling strength of node i can be written as

$$d_{out}^i = \sum_{j=1}^{N} A_{ij} k_i^{\alpha} = k_i^{\alpha} \sum_{j=1}^{N} A_{ij} = k_i^{\alpha} k_i = k_i^{\alpha+1}.$$
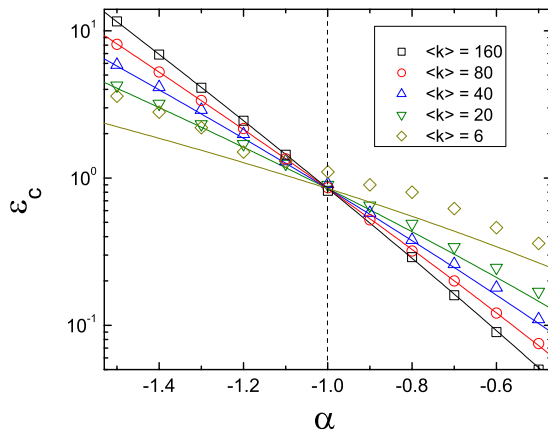
We have

FIG. 4. (Color online) For asymmetric coupling scheme, critical global coupling strength ε_c vs the weighting parameter α for different average degree $\langle k \rangle$. As for the case of symmetric coupling, two distinct regimes exist: (i) $\alpha < -1.0$, the abnormal synchronization regime and (ii) $\alpha > -1.0$, the normal regime. Data points are from simulations and the curves are from analytical predictions Eq. (22). Other network parameters are the same as those in Fig. 1.

$$\langle d_{\text{in}} d_{\text{out}} \rangle = \left\langle \frac{k_i \langle k^{\alpha+1} \rangle}{\langle k \rangle} \cdot k_i^{\alpha+1} \right\rangle$$

$$= \left\langle \frac{k_i^{\alpha+2} \langle k^{\alpha+1} \rangle}{\langle k \rangle} \right\rangle = \frac{\langle k^{\alpha+2} \rangle \langle k^{\alpha+1} \rangle}{\langle k \rangle}. \tag{20}$$

The quantity η_1 in Eq. (5) is given by

$$\eta_1 = \frac{\langle d^{\text{in}} \rangle}{\langle d^{\text{in}} d^{\text{out}} \rangle} = \frac{\langle k \rangle}{\langle k^{\alpha+2} \rangle}. \tag{21}$$

Inserting Eqs. (19)–(21) into Eq. (5), we obtain

$$\varepsilon_c = \beta_1 \eta_1 = \beta_1 \frac{\langle k \rangle}{\langle k^{\alpha+2} \rangle} = \beta_1 \frac{\int_{k_{\text{min}}}^{k_{\text{max}}} (\gamma-1) k_{\text{min}}^{\gamma-1} k^{-\gamma} k \, dk}{\int_{k_{\text{min}}}^{k_{\text{max}}} (\gamma-1) k_{\text{min}}^{\gamma-1} k^{-\gamma} k^{\alpha+2} \, dk}$$

$$= \frac{2}{\pi g(0)} \frac{\alpha - \gamma + 3}{2 - \gamma} \frac{1}{k_{\text{min}}^{\alpha+1}} \frac{N^{(2-\gamma)/(\gamma-1)} - 1}{N^{(\alpha-\gamma+3)/(\gamma-1)} - 1}. \tag{22}$$

Comparison between the theoretical prediction [Eq. (22)] and simulation results is given in Fig. 4. Behaviors similar to those for the symmetric coupling case are observed except that the value of α_c separating the abnormal and the normal synchronization regimes becomes $\alpha_c = -1$. For cases of relatively large average degrees, there is a good agreement between numerics and theory. The slight difference for the case of $\langle k \rangle = 20$ is due to the requirement of reasonably dense connectivity in the mean-field framework, which is better satisfied when the average degree of the network is larger. The value of ε_c for $\alpha = \alpha_c$ is still $2/[\pi g(0)]$, which depends only on the natural frequency distribution of the oscillators. The value of $\varepsilon_c(\alpha_c)$ is thus identical for both the symmetric and the asymmetric coupling cases. It can be regarded as a general quantity characterizing the transition to synchronization in weighted scale-free networks, as it is apparently independent of structural details such as the degree-distribution exponent, the average degree, and the coupling scheme.

IV. EIGENVALUE ANALYSIS FOR CRITICAL COUPLING STRENGTH

A result from Ref. 6 is that the critical coupling strength ε_c at which the transition occurs is determined by the largest eigenvalue of the adjacency matrix for random networks with a prescribed degree distribution,[6]

$$\varepsilon_c = \frac{\beta_1}{\lambda_N}, \tag{23}$$

where β_1 is determined by the frequency distribution $g(\omega)$. It is thus useful to investigate the dependence of $1/\lambda_N$ on the weighting parameter α to gain more support for our results from mean-field analysis. As we will show, the eigenvalue approach suggests strongly the existence of the abnormal and normal synchronization regimes and a crossover point separating the two regimes. The eigenvalue approach for the onset of synchronization is, however, restricted to cases where the mean-field treatment is meaningful as the underlying networks are randomly constructed with some prescribed degree distribution. For standard scale-free networks generated by the preferential-attachment mechanism, although nodes are not randomly connected, the degree-degree correlation among nodes is weak, so the mean-field approximation is still valid. In this case, results from the eigenvalue analysis and from the mean-field theory agree with each other.

The elements of the weighted adjacency matrix C are given by $C_{ij} = A_{ij} w_{ij}$ for $i \neq j$ and $C_{ii} = 0$ otherwise. For the symmetric coupling case, for $\alpha > -0.5$, the corresponding weighted networks are highly heterogeneous. In this case, λ_N can be obtained by considering the square of the weighted adjacency matrix C^2. The largest eigenvalue λ_N' of the matrix C^2 is determined by the largest diagonal term, according to the nondegenerate perturbation theory.[12,13] The diagonal terms of C^2 are given by

$$C_{ii}^2 = \sum_{j=1}^{N} A_{ij} w_{ij} A_{ij} w_{ji} = k_i^{2\alpha+1} \sum_{k'=k_{\text{min}}}^{k_{\text{max}}} P(k'|k_i) k'^{2\alpha}$$

$$= \frac{k_i^{2\alpha+1} \langle k^{2\alpha+1} \rangle}{\langle k \rangle}. \tag{24}$$

We thus have $\lambda_N' = \max_i \{C_{ii}^2\}$ and $\lambda_N = \sqrt{\lambda_N'}$.

For $\alpha < -0.5$, the total local coupling strength d is more homogeneous and, hence, λ_N can be obtained by using the random matrix theory.[14] In particular, λ_N is determined by the maximum value of d to which nodes of the lowest degree contribute, i.e.,

$$\lambda_N \approx d_{\text{max}} = \sum_{j=1}^{N} A_{ij} k_{\text{min}}^{\alpha} k_j^{\alpha}. \tag{25}$$

Summarizing results for both cases, we have

$$\lambda_N \approx \begin{cases} \sqrt{k_{\text{max}}^{2\alpha+1} \langle k^{2\alpha+1} \rangle / \langle k \rangle}, & \alpha > -0.5 \\ k_{\text{min}}^{\alpha+1} \langle k^{\alpha+1} \rangle / \langle k \rangle, & \alpha < -0.5, \end{cases} \tag{26}$$

where k_{max} can be obtained by averaging over different network realizations, and $\langle k^{\alpha+1} \rangle$ and $\langle k \rangle$ are given by Eq. (13). A comparison of results from Eq. (26) and from simulation is shown in Fig. 5. We see that, except for the region around
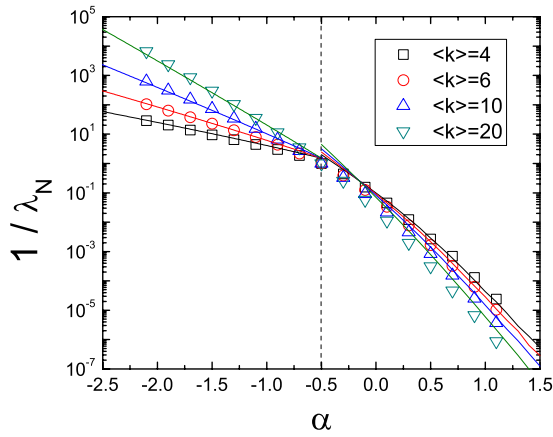
FIG. 5. (Color online) For an ensemble of weighted, symmetrically coupled scale-free networks of $N=1500$ nodes, reciprocal of the largest eigenvalue of the weighted adjacency matrix as a function of α for different values of $\langle k \rangle$. Note that the average degrees are quite small. Data points are obtained by numerical simulations, where each point is the result of averaging over 20 random network realizations, and curves are predicted by Eq. (26).

FIG. 6. (Color online) For weighted, asymmetrically coupled scale-free networks, the quantity $1/\lambda_N$ vs α for different values of the average degree $\langle k \rangle$. Data points are obtained by numerical simulations and curves are predicted by Eq. (27). Other parameters are the same as those in Fig. 5.

$\alpha=-0.5$, there is a reasonable agreement between analytical and numerical results. The interesting feature is the persistent existence of the abnormal and normal synchronization regimes, and the crossover point separating them at which the network synchronizability is apparently independent of, among others, the average degree of the network.

For the asymmetric coupling case, λ_N can be obtained in a similar way. In particular, for $\alpha > -1.0$, we have

$$C_{ii}^2 = \sum_{j=1}^{N} A_{ij} k_i^\alpha k_j^\alpha = k_i^{\alpha+1} \langle k^{\alpha+1} \rangle / \langle k \rangle.$$

For $\alpha < -1.0$, we have

$$d_i = \sum_{j=1}^{N} A_{ij} k_j^\alpha = k_i \langle k^{\alpha+1} \rangle / \langle k \rangle.$$

We thus have

$$\lambda_N = \begin{cases} \sqrt{k_{max}^{\alpha+1} \langle k^{\alpha+1} \rangle / \langle k \rangle}, & \alpha > -1.0 \\ k_{min} \langle k^{\alpha+1} \rangle / \langle k \rangle, & \alpha < -1.0. \end{cases} \quad (27)$$

Figure 6 shows $1/\lambda_N$ as a function of α for the asymmetric coupling scheme for weighted, sparse scale-free networks. There is a reasonable agreement between theoretical and numerical results. The key feature of Fig. 6 is similar to that of Fig. 5, i.e., the existence of the abnormal and normal synchronization regimes and a crossover point separating the two regimes.

V. COMPARISON WITH SYNCHRONIZATION IN NETWORKS OF IDENTICAL OSCILLATORS

For comparison with the results concerning the onset of synchronization in the Kuramoto networks, we consider synchronization in networks of identical oscillators[1] for both coupling schemes, which can, in general, be described by
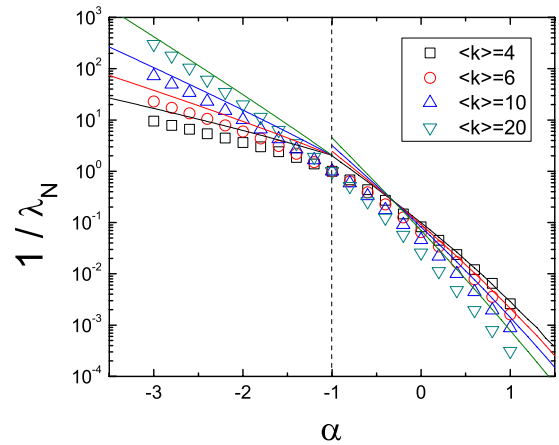
$$\frac{d\mathbf{x}_i}{dt} = \mathbf{F}(\mathbf{x}_i) + \varepsilon \sum_{j=1}^{N} G_{ij} \mathbf{H}(\mathbf{x}_j), \quad (28)$$

where $\mathbf{H}(x)$ is a linear coupling function, ε is the global coupling parameter, and $\mathbf{G}$ is the coupling matrix underlying the network topology. The matrix $\mathbf{G}$ satisfies the condition $\sum_{j=1}^{N} G_{ij} = 0$ for any i, where N is the network size. The variational equations are

$$\frac{d\delta\mathbf{x}_i}{dt} = \mathbf{DF}(\mathbf{s}) \cdot \delta\mathbf{x}_i - \varepsilon \sum_{j=1}^{N} G_{ij} \mathbf{DH}(\mathbf{s}) \cdot \delta\mathbf{x}_j, \quad (29)$$

where $\mathbf{DF}(\mathbf{s})$ and $\mathbf{DH}(\mathbf{s})$ are the Jacobian matrices of the corresponding vector functions evaluated at the synchronization state $\mathbf{s}(t)$. Diagonalizing the coupling matrix $\mathbf{G}$ yields a set of eigenvalues $\{\Lambda_i, i=1, \ldots, N\}$ and the corresponding normalized eigenvectors are denoted by $e_1, e_2, \ldots, e_N$. The eigenvalues are real and non-negative and can be sorted as $0 = \Lambda_1 < \Lambda_2 \leq \cdots \leq \Lambda_N$. The smaller the ratio Λ_N/Λ_2, the stronger the synchronizability of the network.[1]

Figure 7 shows the eigenratio Λ_N/Λ_2 as a function of α for both symmetric and asymmetric coupling schemes. One can see that the synchronizability of identical oscillators is different from that of the Kuramoto network. In particular, there are no crossover behavior and abnormal synchronization regime for both coupling schemes. Instead, the synchronizability is optimized for $\alpha=-1$, and higher connection density $\langle k \rangle$ leads to stronger synchronizability. In this case, our coupling schemes are equivalent to those studied in Ref. 2, and our results are consistent with previously obtained results. The different behaviors between the onset of synchronization in the Kuramoto network and the stability of synchronization state in networks of identical oscillators can partly be explained by the eigenvalue approach. As we have seen, the onset of synchronization in the Kuramoto network is determined by the largest eigenvalue of the adjacency matrix with zero diagonal elements, whereas the synchronizability of networks of identical oscillators is determined by the ratio of the largest and the second lowest eigenvalues of the coupling matrix. From a physical point of view, at the
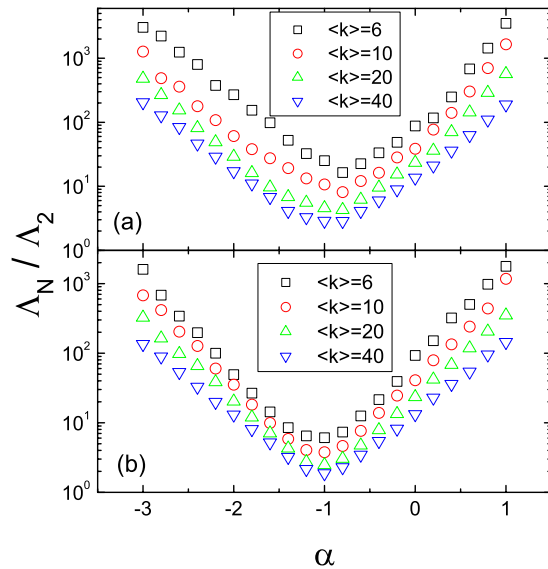
FIG. 7. (Color online) For (a) symmetric coupling scheme and (b) asymmetric coupling scheme, ratio of the largest eigenvalue and the second lowest eigenvalue of the coupling matrix as a function of α for different average degree $\langle k \rangle$ of scale-free networks of $N = 2000$ nodes. Each data point is the results of averaging over 20 random network realizations.

onset of synchronization, partial synchronization emerges from a completely disordered state, while the synchronizability in networks of identical oscillators describes the stability of synchronization state with respect to perturbation. Hence, it is not unreasonable that the emergence of partial synchronization can exhibit quite distinct behaviors.

VI. CONCLUSIONS

In this paper, we have investigated the onset of synchronization in weighted scale-free networks using the Kuramoto model as the platform. We have considered both symmetrical and asymmetrical coupling schemes. Our focus is on the effect of the weighting scheme, characterized by the weighting parameter α, on ε_c, the critical global coupling strength required for coherence in the network to set in. For networks of relatively large values of the average degree, the mean-field theory has been used, which is the standard theoretical tool for treating Kuramoto networks. We have also studied the onset of synchronization in terms of the eigenvalue approach.

Our findings can be summarized as follows. Regardless of the coupling scheme, for weighted scale-free networks there exist two regimes with opposite synchronization behaviors. In the normal regime, the network's ability to synchronize can be enhanced by increasing the number of links in the network, while the opposite behavior occurs in the abnormal regime. A striking phenomenon is that, in the vicinity of the point separating the two regimes, network synchronization has little dependence on the average degree. That is, no matter how the number of links is changed in the network, insofar as the network is connected, the synchronization dynamics are invariant in the sense that the value of ε_c

at the separating point does not depend on details such as the link density and the degree exponent. In fact, the value of ε_c is determined only by the natural frequencies of oscillators, which are fixed when the networked dynamical system is initially defined. These results indicate that weighting can play a quite counterintuitive role in network synchronization. Understanding the effects of coupling weights on synchronization in large-scale complex networks has been an active area of ongoing research. Our work has provided some insights into the issue that may be useful for understanding synchronization-related phenomena in various complex physical, biological, and technological systems.

[1] L. F. Lago-Fernández, R. Huerta, F. Corbacho, and J. A. Sigüenza, Phys. Rev. Lett. **84**, 2758 (2000); M. B. Barahona and L. M. Pecora, *ibid.* **89**, 054101 (2002); X. F. Wang and G. Chen, Int. J. Bifurcation Chaos Appl. Sci. Eng. **12**, 187 (2002); IEEE Trans. Circuits Syst., I: Regul. Pap. **49**, 54 (2002); X. F. Wang, Int. J. Bifurcation Chaos Appl. Sci. Eng. **12**, 885 (2002); M. Timme, F. Wolf, and T. Geisel, Phys. Rev. Lett. **89**, 258701 (2002); T. Nishikawa, A. E. Motter, Y.-C. Lai, and F. C. Hoppensteadt, *ibid.* **91**, 014101 (2003); J. Ito and K. Kaneko, Phys. Rev. E **67**, 046226 (2003); F. M. Atay, J. Jost, and A. Wende, Phys. Rev. Lett. **92**, 144101 (2004); Y. Moreno and A. F. Pacheco, Europhys. Lett. **68**, 603 (2004); P. G. Lind, J. A. C. Gallas, and H. J. Herrmann, Phys. Rev. E **70**, 056207 (2004); L. Huang, K. Park, Y.-C. Lai, and K. Yang, Phys. Rev. Lett. **97**, 164101 (2006); C.-Y. Yin, W.-X. Wang, G. Chen, and B.-H. Wang, Phys. Rev. E **74**, 047102 (2006); C.-Y. Yin, B.-H. Wang, W.-X. Wang, and G.-R. Chen, *ibid.* **77**, 027102 (2008).
[2] A. E. Motter, C. Zhou, and J. Kurths, Phys. Rev. E **71**, 016116 (2005); M. Chavez, D.-U. Hwang, A. Amann, H. G. E. Hentschel, and S. Boccaletti, Phys. Rev. Lett. **94**, 218701 (2005); C. Zhou, A. E. Motter, and J. Kurths, *ibid.* **96**, 034101 (2006); T. Nishikawa and A. E. Motter, Phys. Rev. E **73**, 065106(R) (2006).
[3] Y. Kuramoto, *Chemical Oscillations, Waves and Turbulence* (Springer-Verlag, Berlin, 1984).
[4] S. H. Strogatz, Physica D **143**, 1 (2000).
[5] J. A. Acebrón, L. L. Bonilla, C. J. P. Vicente, F. Ritort, and R. Spigler, Rev. Mod. Phys. **77**, 137 (2005).
[6] J. G. Restrepo, E. Ott, and B. R. Hunt, Phys. Rev. E **71**, 036151 (2005); Chaos **16**, 015107 (2006).
[7] S. Guan, X. Wang, Y.-C. Lai, and C.-H. Lai, Phys. Rev. E **77**, 046211 (2008).
[8] A.-L. Barabási and R. Albert, Science **286**, 509 (1999).
[9] A. Barrat, M. Barthélemy, R. Pastor-Satorras, and A. Vespignani, Proc. Natl. Acad. Sci. U.S.A. **101**, 3747 (2004); P. J. Macdonald, E. Almaas, and A.-L. Barabási, Europhys. Lett. **72**, 308 (2005).
[10] T. Ichinomiya, Phys. Rev. E **70**, 026116 (2004).
[11] J. Gómez-Gardeñes, Y. Moreno, and A. Arenas, Phys. Rev. Lett. **98**, 034101 (2007).
[12] T. Kato, *Perturbation Theory for Linear Operators* (Springer-Verlag, Berlin, 1995).
[13] D.-H. Kim and A. E. Motter, Phys. Rev. Lett. **98**, 248701 (2007).
[14] E. P. Wigner, Ann. Math. **53**, 36 (1951); T. A. Brody, J. Flores, J. B. French, P. A. Mello, A. Pandey, and S. S. M. Wong, Rev. Mod. Phys. **53**, 385 (1981).